APEM journal
Advances in Production Engineering & Management **ISSN 1854-6250**
Volume 17 | Number 2 | June 2022 | pp 193–204 Journal home: apem-journal.org
https://doi.org/10.14743/apem2022.2.430 Original scientific paper

Ultrasonic abrasive polishing of additive manufactured parts: An experimental study on the effects of process parameters on polishing performance

Liu, X.[a], Wang, J.[a,*], Zhu, J.[a], Liew, P.J.[b], Li, C.[c], Huang, C.[d]

[a]Marine Engineering College, Dalian Maritime University, Ganjingzi District, Dalian, P.R. China
[b]Fakulti Kejuruteraan Pembuatan, Universiti Teknikal Malaysia Melaka, Hang Tuah Jaya, Durian Tunggal, Melaka, Malaysia
[c]Xinyu Key Laboratory of Materials Technology and Application for Intelligent Manufacturing, Xinyu University, P.R. China
[d]College of Marine Engineering, Jimei University, Fujian, P.R. China

A B S T R A C T

The rough surface of metal parts produced by the powder-based layered Additive Manufacturing (AM) technology such as Selective Laser Melting (SLM) is an important problem that needs to be solved. This study introduces obvious improvements in the surface quality of the AM parts by means of ultrasonic abrasive polishing (UAP), which uses cavitation collapse and micro-cut of abrasive particles for finishing surfaces. Experiments were conducted using the orthogonal experimental design method with an $L_9(3^4)$ orthogonal array to investigate the effects of ultrasonic power, machining time, abrasive particle size, and particle concentration on surface roughness *Ra* and material removal rate (MRR). The wear of the abrasive particles in the slurry was also studied. IN625 nickel-based alloy specimen manufactured by Selective Laser Melting (SLM) was chosen as the target workpiece. The results show that when the ultrasonic output power was too high, both surface quality and machining efficiency were deteriorated. And the surface roughness *Ra* was not further improved by just increasing the machining time. Severe cavitation erosion occurred in the polishing process and created leftover pits on the workpiece surface, which has a large influence on *Ra*. The size and amount of the abrasive particles should be within a certain range, which is helpful for material removal and improving the polishing performance. The work is useful for studying the influential process parameters involved in UAP and finding out the appropriate conditions.

A R T I C L E I N F O

Keywords:
Additive manufacturing;
3D printing;
Selective laser melting (SLM);
Ultrasonic abrasive polishing;
Process parameters;
Surface roughness;
Material removal rate;
Orthogonal array tests

**Corresponding author:*
wjs@dlmu.edu.cn
(Wang, J.)

Article history:
Received 19 January 2022
Revised 14 August 2022
Accepted 21 August 2022

1. Introduction

Additive Manufacturing (AM) technology is a process of joining materials layer by layer to make parts based on a pre-designed three-dimensional model data, which is distinguished from traditional subtractive machining techniques [1]. The manufactured components have high dimensional accuracy and long-term dimensional stability [2, 3] Therefore, the AM technology greatly reduces waste material, part weight, and production time. In addition, manufacturing components with no geometric limitations makes it attractive in various fields such as automotive, aerospace, and medicine [4-8].

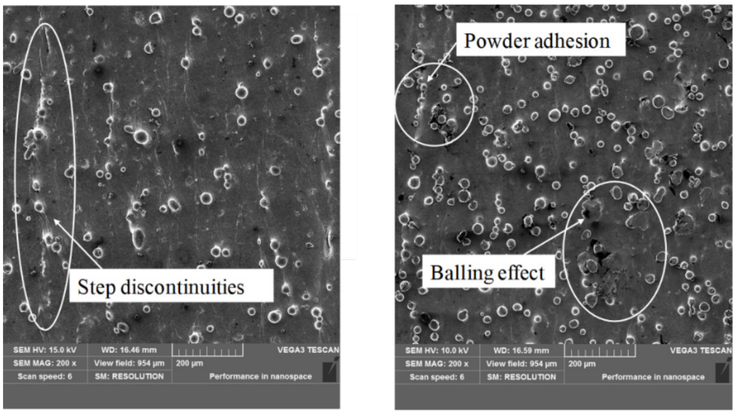

Fig. 1 Stair-stepping effect, balling effect, and powder adhesion in SLM

A laser beam can be focused to a small size which makes the energy density high and can minimize the molten pool and heat-affected zone. Therefore, lasers have been widely utilized in AM processes, especially for the metallic materials with high melting points [9-12]. The laser-based AM processes are classified into two categories [13]. One is the laser-based directed energy deposition (L-DED), where the material can be either wire or powder, and is melted and deposited simultaneously. The other one is the laser-based powder bed fusion (L-PBF), where the laser source selectively melts metallic powders layer by layer. Even though the L-DED has faster built speeds, the L-PBF is more popular due to its better manufacturing capability for producing compact features with greater geometrical accuracy and high specific strength [10, 12].

Selective laser melting (SLM) and Selective laser sintering (SLS) are typical L-PBF technologies. SLS technology has relatively low strength sintered parts. In addition, the mechanical properties and forming accuracy of SLS sintered parts are lower than that of SLM due to voids in process entities [14]. SLM acts as one of the most popular AM processes for metallic materials in industry now. However, the surface roughness of the SLM parts is still too high for direct uses. In the SLM process, stair-stepping effect, balling effect, and powder adhesion [15-18] are the three main factors leading to the poor quality as shown in Fig. 1. These not only affect the aesthetics, but also greatly limits the functional performance of the parts including fatigue life and friction properties [19].

To improve the surface quality of AM parts for practical uses, various post-process finishing techniques are implemented [20]. Today, manual polishing is still the main polishing method for AM parts, but it needs long operating time and high labor costs, and the accuracy is dependent on the experience of the personnel. Chemical polishing, electrochemical polishing, laser polishing, and abrasive flow machining have shown their capabilities in finishing AM parts [21-23]. However, they have their respective advantages and shortcomings when applied to surface polishing of AM parts. The larger thermal damage caused by laser polishing leads to the deformation of metal parts more easily. In the same way, chemical polishing causes great chemical damage. While electrochemical polishing is not suitable for polishing metal parts with deep inner holes. Abrasive flow machining is potential for surface finishing of internal channels, but it still has the limitations include damage to thin-walled structures due to excessive pumping pressures and abrasive contamination in the internal channels.

The principle of ultrasonic abrasive polishing, abbreviated as UAP here, was proved effective in improving surface quality of AM parts in some recent studies [21, 24-26]. In this process, the materials are removed by the combination of cavitation and micro-cut of abrasive particles, which is feasible for finishing various AM parts with complex external and internal surfaces. Mass and dimensional losses are only significant for initially rough surfaces with numerous surface irregularities. Therefore, UAP has the potential to finish the surface without alteration of the original AM dimensions, which distinguishes it from other surface finishing techniques. Nevertheless, the machining capability of UAP for finishing AM surfaces is not totally understood. Many input parameters exist in UAP which would influence the polishing performance, and there is a lack of systematic study on this. In this study, UAP experiments of SLM manufactured

IN625 alloy specimen were conducted using the orthogonal experimental design method with an $L_9(3^4)$ orthogonal array to investigate the effects of ultrasonic power, machining time, abrasive size, and abrasive concentration on polishing results. The work is useful for studying the influential process parameters involved in UAP and improving the machining performance.

2. Basic principle of ultrasonic abrasive polishing (UAP)

UAP uses an ultrasonic tool (horn) in conjunction with abrasive particles suspended in a liquid slurry for surface polishing, the ultrasonic tool tip should be at a specific distance away from the specimen surface to prevent a contact between them. According to the previous studies, three main material removal modes in the polishing process were concluded [25, 27] and schematically shown in Fig. 2. They include:

- Cavitation erosion from the abrasive slurry, which is effective for removing partially melting powders on the AM surfaces.
- Abrasion by the impact of the abrasive particles against the workpiece accelerated by the force of cavitation collapse.
- Small-scale material removal by high frequency impact of abrasive particles excited by ultrasonic vibration of the tool.

In addition, the cavitation effect is helpful for the circulation of abrasives and chip removal of the workpiece materials, which facilitate the material removal in UAP.

The cavitation is mainly influenced by ultrasonic amplitude, ultrasonic frequency, and physical parameters of the liquid. Generally, ultrasonic frequency ranged from 20-40 kHz is appropriate for cavitation. The cavitation intensity increases with the increase of the ultrasonic amplitude. And an increase of the liquid viscosity would suppress the cavitation. On the other hand, the frequency and intensity of the abrasive impact would also be influenced by the input ultrasonic parameters and the characteristics of the particles.

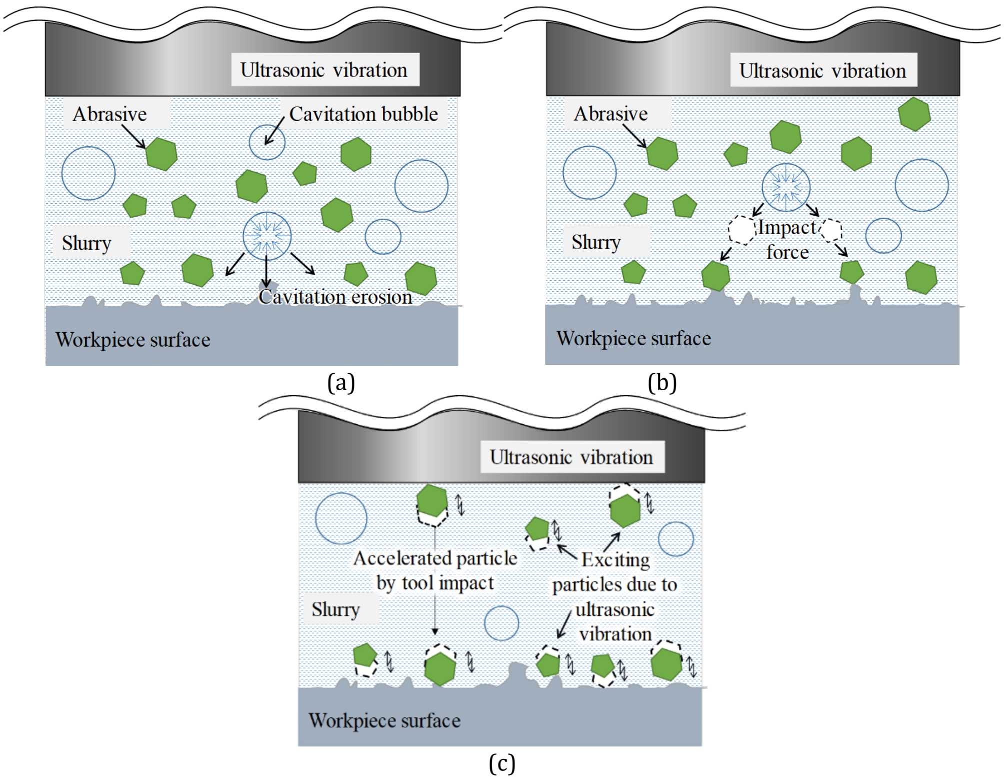

Fig. 2 Schematic view of material removal in UAP: (a) cavitation erosion, (b) abrasive impact accelerated by cavitation collapse, (c) abrasive impact excited by ultrasonic vibration of the tool

Therefore, both the settings of the ultrasonic parameters and the composition of the slurry are important for the material removal in UAP, and accordingly influence the polishing efficiency and the surface quality. In the following sections, UAP experiments are introduced, discussions are also conducted based on the experimental results and previous studies.

3. Materials and methods

3.1 Materials

The slurry composed of silicon carbide abrasive particles and purified water. The IN625 specimen was a cube with a side length of 20 mm, which was manufactured by a SLM equipment (FARSOON) with the scanning speed of 7.6 m/s. The metal powder size ranges from 15 µm to 53 µm. The powder-bed depth is 0.1 mm, and the material parameters are illustrated in Table 1. Surfaces built at 90° orientation were treated with UAP process.

Table 1 Material parameters

Element	C	Si	Mn	S	P	Cr	Ni	Mo	Al	Ti	Nb+Ta	Co	Fe
wt %	≤ 0.1	≤ 0.5	≤ 0.5	≤ 0.015	≤ 0.015	20.0-23.0	≥ 58.0	8.8-10.0	≤ 0.4	≤ 0.4	3.15-4.15	< 1.0	< 5.0

3.2 Experimental setup

An ultrasonic generator with the output power ranging from 800-1800 W (Ningbo Scientz Biotechnology) was used in this work. The frequency is 19.5-20.5 kHz. The diameter of the horn tip is 25 mm. The ultrasonic amplitude can be adjusted purposely by changing the output power.

3.3 Design of experiments

In this study, the surface roughness *Ra* and the material removal rate (MMR) were used for evaluating the polishing performance of UAP. To obtain the appropriate condition covering a wide range of factors in a more efficient way, the orthogonal experimental design was applied to reduce the number of experiments. Table 2 lists the specific conditions of an $L_9(3^4)$ orthogonal array used in this work, corresponding to four factors of three levels. As shown in Table 2, three levels of ultrasonic power were 900, 1200 and 1500 W. Three levels of machining time were 10 min, 20 min and 30 min. Three levels of abrasive size were 800, 1200, and 2000 grit sizes. Three levels of abrasive concentration were 5 %, 10 % and 15 %.

Table 2 Experimental design using the L9 orthogonal array

Experimental number	Factors			
	A (Ultrasonic power)	B (Machining time)	C (Abrasive size)	D (Abrasive concentration)
1	900	10	800	5
2	900	20	1200	10
3	900	30	2000	15
4	1200	10	1200	15
5	1200	20	2000	5
6	1200	30	800	10
7	1500	10	2000	10
8	1500	20	800	15
9	1500	30	1200	5

The orthogonal experimental results were studied with the range analysis, which is a statistical method to determine the sensitivity of the factors and to obtain the optimal process conditions. The analyzing process of range analysis is as follows:

$$k_{Xm} = K_{Xm} / 3 \quad (1)$$

$$R = \max(k_{X1}, k_{X2}, k_{X3}) - \min(k_{X1}, k_{X2}, k_{X3}) \quad (2)$$

K_{Xm} and k_{Xm} means the sum and the average value of the experimental results of factor *X* with level *m*. *R* means the influence degree of the factor *X*, and the higher the value *R* is, the greater the influence degree of factor *X* is. The tendency charts showing the influence of each parameter on the surface roughness and the MRR were also drawn based on the range analysis.

3.4 Experimental procedure

As shown in Fig. 3, the workpiece to be polished was fixed in a container filled with the abrasive slurry. The ultrasonic tool was immersed in the slurry, the distance between the tool tip and the workpiece was adjusted to guarantee efficient polishing and prevent direct contact between the two. Meanwhile, cooling system was applied during the process to avoid a drastic increase in temperature of the horn. Repeated polishing experiments were conducted for each condition as shown in Table 2. After polishing, the surface roughness was tested by a hand-held roughness meter with the measurement accuracy of 0.002 μm (Mitutoyo), and the surface was observed with a scanning electron microscope (TESCAN). Due to the high standard deviations of AM surface, as least as 5 measurements of each specimen were conducted to calculate the average *Ra* value. The weight of the workpiece before and after polishing was measured by an electronic balance with the measurement accuracy of 0.1 mg. Thus, the MRR can be calculated as the difference of weight over the polishing time. In addition, the particle size distribution before and after machining was examined by a particle size analysis device (Mastersizer 3000, Malvern Panalytical) to study the wear of abrasive particles.

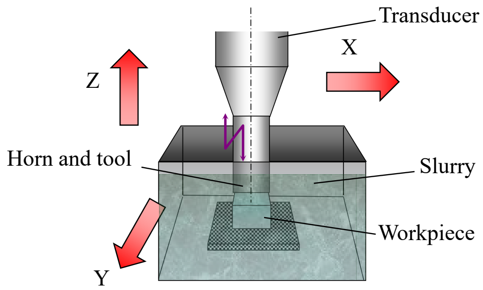

Fig. 3 Schematic view of the experimental process

4. Results and discussions

The obtained surface roughness *Ra* and MRR after ultrasonic polishing experiments are as shown in Table 3. The initial average *Ra* of the target SLM surface is 9.48 μm. After polishing, the surface roughness was decreased obviously ranging from 5.01 μm to 6.80 μm. The MRR ranges from 1.14 mg/min to 3.0 mg/min.

Table 3 Results of surface roughness and MRR

Experimental number	Surface roughness *Ra* (μm)	MMR (mg/min)
1	5.58	2.40
2	5.92	2.15
3	6.05	1.86
4	6.20	1.84
5	5.66	2.71
6	6.22	1.57
7	5.01	3.00
8	6.80	1.14
9	6.20	1.57

Range analysis results of surface roughness and MRR were presented in Table 4 and Table 5, respectively. K_j and k_j represents the sum and average value of the measurement results of the roughness and the MRR for each factor (each column) with level *j*, *j* = 1, 2, 3, respectively. The results show that the main influence factor on surface roughness is abrasive concentration, and the influence order of different process parameters on *Ra* is: abrasive concentration > abrasive size > machining time > ultrasonic power based on the value *R*. The main influence factor on MRR is abrasive size, and the influence order of the parameters is: abrasive size > machining time > abrasive concentration > ultrasonic power using the same analysis method. In this work, the surface roughness value is required to be as small as possible, which means the surface quality is improved. On the other hand, the MRR should be high, which is important to increase the machining efficiency. When the combination of the four process parameters is ultrasonic power at 900 W, machining time of 10 min, grit size at 2000, and abrasive concentration at 10 %, the analysis results show smallest *Ra* value (the corresponding level of minimum *k* for each factor) and highest MRR (the corresponding level of maximum *k* for each factor).

Table 4 Range analysis on surface roughness

	Ultrasonic power (W)	Machining time (min)	Abrasive size (μm)	Abrasive concentration (% wt)
K_1	17.55	16.79	18.60	17.44
K_2	18.08	18.38	18.32	17.15
K_3	18.01	18.47	16.72	19.05
k_1	5.850	5.597	6.200	5.813
k_2	6.027	6.127	6.107	5.717
k_3	6.003	6.157	5.573	6.350
R	0.177	0.560	0.627	0.633
Order of priority	Abrasive concentration > Abrasive size > Machining time > Ultrasonic power			
Optimal level	900	10	2000	10
Optimal combination	900 W, 10 min, 2000 grit, 10 %			

Table 5 Range analysis on MRR

	Ultrasonic power (W)	Machining time (min)	Abrasive size (μm)	Abrasive concentration (% wt)
K_1	6.41	7.24	5.11	6.68
K_2	6.12	6.00	5.56	6.72
K_3	5.71	5.00	7.57	4.84
k_1	2.137	2.413	1.703	2.227
k_2	2.040	2.000	1.853	2.240
k_3	1.903	1.667	2.523	1.613
R	0.233	0.747	0.820	0.627
Order of priority	Abrasive size > Machining time > Abrasive concentration > Ultrasonic power			
Optimal level	900	10	2000	10
Optimal combination	900 W, 10 min, 2000 grit, 10 %			

4.1 Effects of ultrasonic power

Fig. 4 shows the effects of ultrasonic power on surface roughness and MRR. When the output power of the ultrasonic generator was 900 W, better surface roughness *Ra* and larger MRR were obtained compared to 1200 W and 1500 W. Based on our former research [25], when the ultrasonic power is among 400 W to 600 W, the surface becomes smoother with the increase of ultrasonic power. It is considered that with the increase of ultrasonic power, the cavitation intensity is enhanced which strengthens the cavitation erosion effects on the work surface and accordingly facilitates the removal of partially melted powders. In addition, abrasion against the workpiece due to the impact of abrasive particle that accelerated by cavitation collapse is also enhanced, so irregularities on the initially rough AM surfaces can be gradually smoothed. However, in this work, it is found that a too high ultrasonic power deteriorates both the surface quality and the machining efficiency. Existed studies have shown that the cavitation erosion effects on a solid surface increase with ultrasonic power up to a threshold and then decrease [28, 29]. The presence of a maximum in the ultrasonically enhanced erosion effects with increasing power is attributed to a peak in the cavitation intensity, which is supposed to increase with the enhancement of ultrasonic power if the collapse time allows the cavitation bubble to grow [30, 31]. Therefore, the condition produces maximum of cavitation erosion effects must be a function of power as well as frequency. On the other hand, it is commonly believed that the horn amplitude (here is controlled by the output power) has a significant effect on ultrasonic machining [32]. In this work, the output power has minimal impact on *Ra* and MRR compared to the other factors, which may be related to the choice of the three high output power levels.

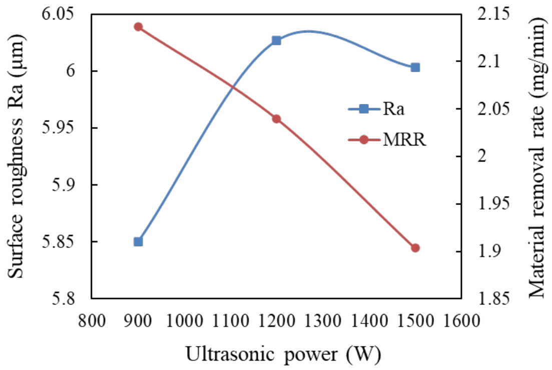

Fig. 4 Effects of ultrasonic power on surface roughness and MRR

The wear of abrasive particles under 900 W and 1500 W were compared by examining particle size distribution before and after polishing process. Other conditions are the same: 2000 grit size abrasive particles, 5 % abrasive concentration, machining time of 20 min. The results are shown in Fig. 5. The maximum particle size that can be detected becomes smaller as indicated with the ellipse marks after polishing (maximum value shifted to the left). The mean particle size before polishing was found to be 8.98 μm, according to the measurement report. After polishing with 900 W and 1500 W, the mean particle size reduces to 8.74 μm and 8.16 μm, respectively. The wear of abrasive particles is increased due to the stronger cavitation effect at higher ultrasonic power. Therefore, more motion energy of the abrasive particles was consumed in the wear between the particles but not the material removal of the workpiece when the ultrasonic power was 1500 W, which accordingly influences the polishing efficiency and the surface quality.

Fig. 6(a) shows the typical surface characteristics of the workpiece before polishing, and Fig. 6(b) is the same area after polishing. Obvious improvement of surface quality can be confirmed. The partially melted powders were almost removed as indicated in area A, and some larger discontinuities were also smoothed as shown in area B. On the other hand, tightly attached balls and irregular structures were challenging to be removed. In addition, some leftover pits due to cavitation erosion are found on the polished surface as shown in area C. With the increase of ultrasonic power, severe cavitation erosion may occur, which can leave more such leftover structures on work surface and increase the *Ra* value.

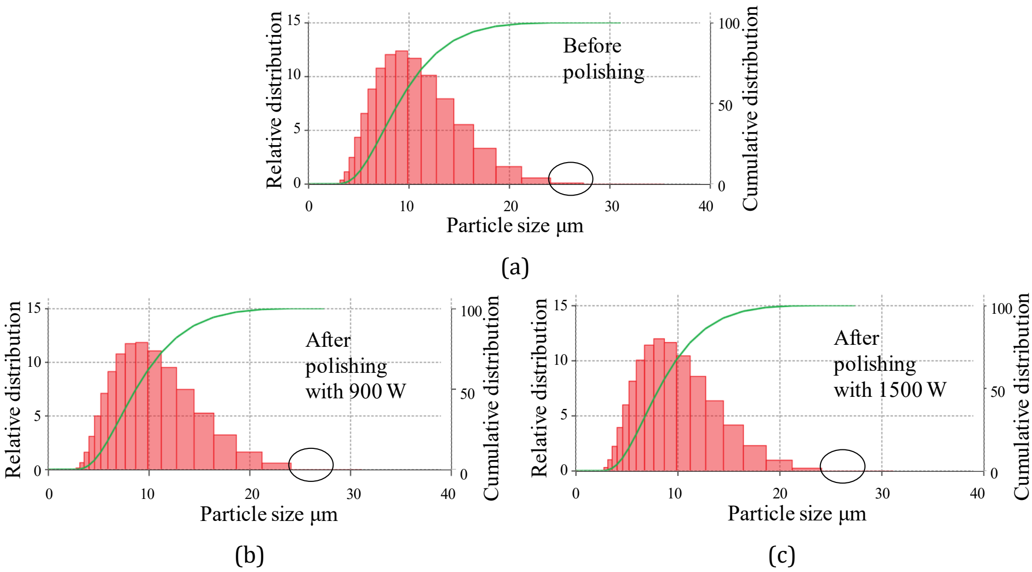

Fig. 5 Particle size distribution before (a) and after polishing with (b) 900 W and (c) 1500 W

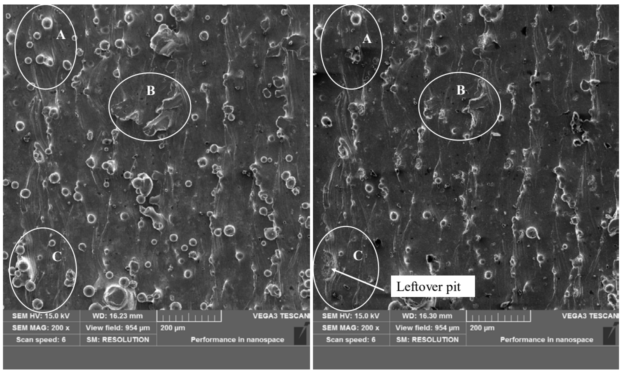

Fig. 6 SEM images of the surfaces: (a) as-manufactured AM workpiece surface; (b) surface after ultrasonic abrasive polishing

Therefore, although the machining capability of UAP could be enhanced at higher power, the increase in wear of abrasives and excessive erosion of surface occur simultaneously, which strongly influences the polishing process. In addition, large number of cavitation bubbles and broken abrasive particles between the horn and the workpiece may play a screening role that inhibits effective cavitation erosion and abrasion of particles against the workpiece at higher power. All these lead to the better surface roughness *Ra* and larger MRR at 900 W than 1200 W and 1500 W in this work.

4.2 Effects of machining time

Fig. 7 shows the effects of machining time on surface roughness *Ra* and MRR. The machining time of 10 min resulted in minimum *Ra* and maximum MRR compared to 20 min and 30 min. At the initial stage of polishing, the partially melted powders were removed quickly, and the peak of material surface was easily to be ground. Therefore, the *Ra* value rapidly reduced, and the MRR was high. With the increase of polishing time, the peak of the surface was smoothed and became flat, which slowed down the MRR. And we found the similar tendency in the previous work [25] that the partially melted powders were predominately removed in the first several minutes and only slight material removal occurred in the remaining machining time. The surface was significantly modified in the initial stage (around several minutes or less) and converge to an equilibrium state.

Normally, the *Ra* should not be worse because more powders and irregular structures might be removed with the increase of the machining time. However, the results show an obvious increase in the *Ra* value after 20 min and 30 min. The workpiece was an AM manufactured part and has its own surface features, large pits may be left on the surface as introduced in area C of Fig. 6 after the removal of tightly attached large balls and irregular structures due to severe cavitation erosion. This has a large effect on the surface roughness *Ra*. In addition, the existence of these pits may further negatively affect the polishing performance because it is easier to deepen the pits under cavitation erosion and abrasive impacts than to flatten them. It seems more necessary to finding out appropriate conditions to facilitate effective polishing action for further reducing the *Ra* value.

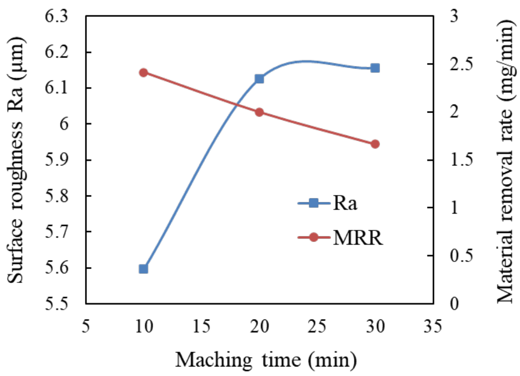

Fig. 7 Effects of machining time on surface roughness and MRR

On the other hand, with the increase of processing time, the wear of abrasive becomes more and more serious, which weakens the grinding capability of abrasive particles. And in the experiments, no new slurry was introduced in the machining area, the continuous high-power ultrasonic work leads to severe wear of abrasive particles and affects the UAP process.

4.3 Effects of abrasive size

Fig. 8 shows the effects of abrasive size on surface roughness *Ra* and MRR. Using abrasive particles of 2000 grit size resulted in minimum *Ra* and maximum MRR compared to 1200 and 800 grit sizes. The abrasive particles act as bubble nucleation sites, compared to smaller particles, the larger particles have larger surface areas to compete for bubble nucleation, so the cavitation erosion against workpiece may be inhibited in the presence of larger particles. Accordingly, material removal process is influenced.

The wear of abrasive particles of 2000 and 800 grit sizes were compared by examining particle size distribution before and after polishing process, respectively. Other conditions are the same: 900 W ultrasonic power, 5 % abrasive concentration, and machining time of 20 min. The results are shown in Fig. 9, the particles become smaller due to the wear for both cases. The mean particle size of 2000 and 800 grit abrasive particles decrease from 8.98 μm and 19 μm to 8.74 μm and 17.7 μm, respectively. A decrease of 2.7 % and 6.8 % in mean particle size for 2000 and 800 grit abrasive particles is confirmed. Therefore, more motion energy was consumed in abrasive broken for larger abrasive particles, and accordingly influences the polishing process. In addition, the larger size particle could act as a physical barrier on the specimen surface to avoid the impact of micro-jets induced by cavitation collapse and affect the material removal [21]. The diameters of the micro-jets are around 10-30 μm [33]. The mean particle size of 1200 and 800 grit abrasive particles are 13.8 μm and 19 μm, respectively, which would screen the micro-jets and inhibit material removal. Therefore, when using abrasives of 1200 and 800 grit sizes, both surface quality and machining efficiency are deteriorated.

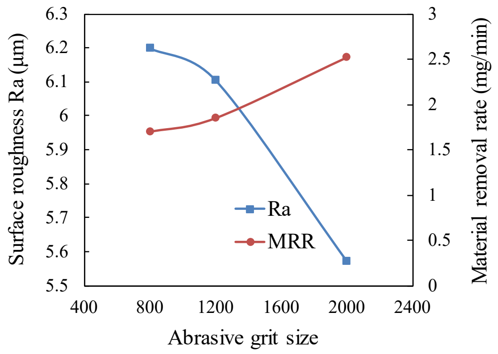

Fig. 8 Effects of abrasive size on surface roughness and MRR

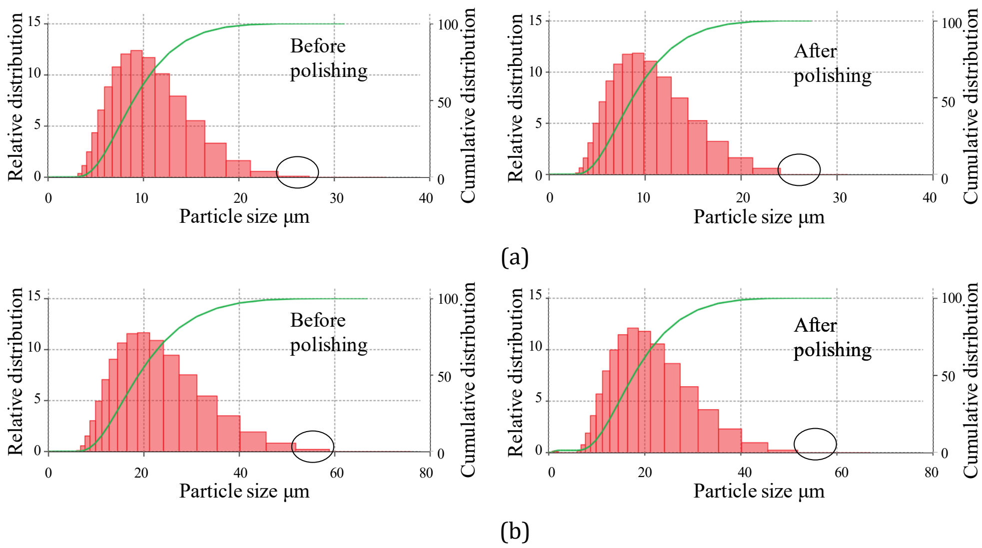

Fig. 9 Particle size distribution before and after polishing: (a) 2000 and (b) 800 grit sizes

4.4 Effects of abrasive concentration

Fig. 10 shows the effects of abrasive concentration on surface roughness *Ra* and MRR. The abrasive concentration at 10 % resulted in minimum *Ra* and maximum MRR compared to 5 % and 15 %. The former studies [21, 25] also showed that the surface roughness is improved with the increase of abrasive concentration in a certain range, then the *Ra* value cannot get better with a further increase in abrasive concentration. And the MRR also showed the same tendency. When the abrasive concentration is too high, the interference between the abrasive particles increases. It is supposed that more motion energy of the abrasive particles would be consumed in the impact between the particles but not the material removal of the workpiece, which would accordingly affect the polishing performance. Furthermore, a large number of abrasive particles would act competing nucleation sites, which may inhibit the cavitation erosion against the workpiece, resulting in the reduction of material removal.

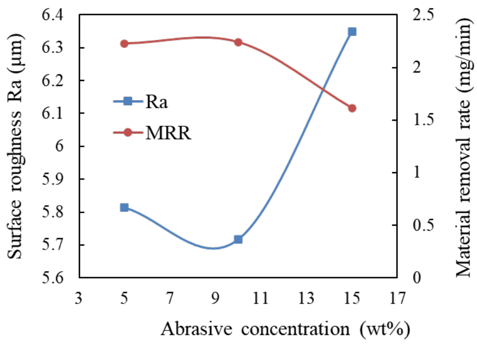

Fig. 10 Effects of abrasive concentration on surface roughness and MRR

5. Conclusion

Since ultrasonic process is cost effective and applicable to the manufacturing of micro-to macro-scale structures, it may lead to new applications in specially designed surface treatment by controlling the process parameters appropriately. In this work, the machining capability of UAP which used ultrasonic cavitation in an abrasive slurry was studied. Polishing experiments on SLM manufactured IN625 alloy specimen were conducted using the orthogonal experimental design method with an $L_9(3^4)$ orthogonal array. Range analysis was performed on the experimental results to investigate the effects of ultrasonic power, machining time, abrasive size, and abrasive concentration on polishing performance. The work is useful for studying the influential process parameters involved in ultrasonic abrasive polishing and optimizing the process parameters. The following conclusions can be drawn:

- When the ultrasonic power is too high, both abrasive wear and cavitation bubbles increase, which may play a screening role that inhibits cavitation erosion and abrasion of particles against the workpiece. Therefore, the surface quality and the machining efficiency would be deteriorated.
- During polishing process, severe cavitation erosion can occur and create leftover pits on the workpiece surface, which has a large influence on *Ra*.
- The AM surface is significantly modified in the initial polishing stage because the partially melted powders and some peak irregular structures are removed.
- Using too large abrasive particles is not helpful for material removal. The larger particles have larger surface areas to compete for bubble nucleation and act as physical barriers on the workpiece surface to inhibit the material removal of the workpiece. And the severe wear of large abrasive particles also influences the polishing performance.
- Both the surface quality and the MRR were improved when the abrasive concentration increased within a certain range. While the abrasive concentration is too high, the interference between the abrasive particles increases, the material removal is suppressed, and the surface quality is also deteriorated.

- Based on the range analysis, the influence order of different process parameters on *Ra* was abrasive concentration > abrasive size > machining time > ultrasonic power, while the influence order of the parameters on MRR was abrasive size > machining time > abrasive concentration > ultrasonic power in this study. When the ultrasonic power, machining time, grit size and abrasive concentration are 900 W, 10 min, 2000 grit size, and 10 %, respectively, the analysis results show smallest *Ra* value and highest MRR.

Funding

This work is supported by China Postdoctoral Science Foundation [Grant no. 2019M651093], the Natural Science Foundation of Liaoning Province (China) [Grant no. 2021-MS-135], Dalian Science and Technology Development Funds of China [Grant no. 2020RQ092], the National Natural Science Foundation of China [Grant no. 51805067], Fundamental Research Funds for the Central Universities of China [Grant no. 3132019366].

Conflicts of Interest

The authors declare no conflict of interest.

References

[1] ASTM International. (2015). ISO/ASTM52900-15 Standard terminology for additive manufacturing-general principles- terminology, West Conshohocken, PA: ASTM International.

[2] Mandić, M., Galeta, T., Raos, P., Jugović, V. (2016). Dimensional accuracy of camera casing models 3D printed on Mcor IRIS: A case study, *Advances in Production Engineering & Management,* Vol. 11, No. 4, 324-332, doi: 10.14743/apem2016.4.230.

[3] Mendricky, R., Soni, R.D. (2022). Geometric stability of parts produced by 3D printing, *Tehnički Vjesnik – Technical Gazette,* Vol. 29, No. 1, 23-29, doi: 10.17559/TV-20191101110214.

[4] Han, X., Zhu, H., Nie, X., Wang, G., Zeng, X. (2018). Investigation on selective laser melting AlSi10Mg cellular lattice strut: Molten pool morphology, surface roughness and dimensional accuracy, *Materials,* Vol. 11, No. 3, Article No. 392, doi: 10.3390/ma11030392.

[5] Calignano, F., Peverini, O.A., Addamo, G., Iuliano, L. (2020). Accuracy of complex internal channels produced by laser powder bed fusion process, *Journal of Manufacturing Processes,* Vol. 54, 48-53, doi: 10.1016/j.jmapro.2020.02.045.

[6] Calignano, F., Manfredi, D., Ambrosio, E.P., Biamino, S., Lombardi, M., Atzeni, E., Salmi, A., Minetola, P., Iuliano, L., Fino, P. (2017). Overview on additive manufacturing technologies, *Proceedings of the IEEE,* Vol. 105, No. 4, 593-612, doi: 10.1109/JPROC.2016.2625098.

[7] Polanec, B., Kramberger, J., Glodež, S. (2020). A review of production technologies and materials for manufacturing of cardiovascular stents, *Advances in Production Engineering & Management,* Vol. 15, No. 4, 390-402, doi: 10.14743/apem2020.4.373.

[8] Patalas-Maliszewska, J., Topczak, M. (2021). A new management approach based on Additive Manufacturing technologies and Industry 4.0 requirements, *Advances in Production Engineering & Management,* Vol. 16, No. 1, 125-135, doi: 10.14743/apem2021.1.389.

[9] Wei, C., Zhang, Z., Cheng, D., Sun, Z., Zhu, M., Li, L. (2021). An overview of laser-based multiple metallic material additive manufacturing: From macro-to micro-scales, *International Journal of Extreme Manufacturing*, Vol. 3, No. 1, Article No. 012003, doi: 10.1088/2631-7990/abce04.

[10] DebRoy, T., Wei, H.L., Zuback, J.S., Mukherjee, T., Elmer, J.W., Milewski, J.O., Beese, A.M., Wilson-Heid, A., De, A., Zhang, W. (2018). Additive manufacturing of metallic components – Process, structure and properties, *Progress in Materials Science,* Vol. 92, 112-224, doi: 10.1016/j.pmatsci.2017.10.001.

[11] Lewandowski, J.J., Seifi, M. (2016). Metal additive manufacturing: A review of mechanical properties, *Annual Review of Materials Research,* Vol. 46, 151-186, doi: 10.1146/annurev-matsci-070115-032024.

[12] Gao, W., Zhang, Y., Ramanujan, D., Ramani, K., Chen, Y., Williams, C.B., Wang, C.C.L., Shin, Y.C., Zhang, S., Zavattieri, P.D. (2015). The status, challenges, and future of additive manufacturing in engineering, *Computer-Aided Design*, Vol. 69, 65-89, doi: 10.1016/j.cad.2015.04.001.

[13] ASTM International. (2013). *Standard Terminology for Additive Manufacturing Technologies,* ASTM International 2013 F2792–12a.

[14] Kozior, T. (2020). Rheological properties of polyamide PA 2200 in SLS technology, *Tehnički Vjesnik – Technical Gazette,* Vol. 27, No. 4, 1092-1100, doi: 10.17559/TV-20190225122204.

[15] Wang, J., Liu, S., Fang, Y., He, Z. (2020). A short review on selective laser melting of H13 steel, *International Journal of Advanced Manufacturing Technology,* Vol. 108, 2453-2466, doi: 10.1007/s00170-020-05584-4.

[16] Strano, G., Hao, L., Everson, R.M., Evans, K.E. (2013). Surface roughness analysis, modelling and prediction in selective laser melting, *Journal of Materials Processing Technology,* Vol. 213, No. 4, 589-597, doi: 10.1016/j.jmatprotec.2012.11.011.

[17] Bhaduri, D., Penchev, P., Batal, A., Dimov, S., Soo, S.L., Sten, S., Harrysson, U., Zhang, Z., Dong, H. (2017). Laser polishing of 3D printed mesoscale components, *Applied Surface Science,* Vol. 405, 29-46, doi: 10.1016/j.apsusc.2017.01.211.
[18] Cabanettes, F., Joubert, A., Chardon, G., Dumas, V., Rech, J., Grosjean, C., Dimkovski, Z. (2018). Topography of as built surfaces generated in metal additive manufacturing: A multi scale analysis from form to roughness, *Precision Engineering,* Vol. 52, 249-265, doi: 10.1016/j.precisioneng.2018.01.002.
[19] Gordon, E.R., Shokrani, A., Flynn, J.M., Goguelin, S., Barclay, J., Dhokia, V. (2016). A surface modification decision tree to influence design in additive manufacturing, In: Setchi, R., Howlett, R., Liu, Y., Theobald, P. (eds.), *Sustainable design and manufacturing 2016. SDM 2016. Smart innovation, systems and technologies, Vol. 52,* Springer, Cham, Switzerland, doi: 10.1007/978-3-319-32098-4_36.
[20] Kumbhar, N.N., Mulay, A.V. (2018). Post processing methods used to improve surface finish of products which are manufactured by additive manufacturing technologies: A review, *Journal of The Institution of Engineers (India): Series C, Mechanical, Production, Aerospace and Marine Engineering,* Vol. 99, 481-487, doi: 10.1007/s40032-016-0340-z.
[21] Tan, K.L., Yeo, S.H. (2020). Surface finishing on IN625 additively manufactured surfaces by combined ultrasonic cavitation and abrasion, *Additive Manufacturing,* Vol. 31, Article No. 100398, doi: 10.1016/j.addma.2019.100938.
[22] Nagalingam, A.P., Yuvaraj, H.K., Yeo, S.H. (2020). Synergistic effects in hydrodynamic cavitation abrasive finishing for internal surface-finish enhancement of additive-manufactured components, *Additive Manufacturing,* Vol. 33, Article No. 101110, doi: 10.1016/j.addma.2020.101110.
[23] Zhao, C., Qu, N., Tang, X. (2021). Removal of adhesive powders from additive-manufactured internal surface via electrochemical machining with flexible cathode, *Precision Engineering,* Vol. 67, 438-452, doi: 10.1016/j.precisioneng.2020.11.003.
[24] Lee, J.-Y., Nagalingam, A.P., Yeo, S.H. (2020). A review on the state-of-the-art of surface finishing processes and related ISO/ASTM standards for metal additive manufactured components, *Virtual and Physical Prototyping,* Vol. 16, No. 1, 68-96, doi: 10.1080/17452759.2020.1830346.
[25] Wang, J., Zhu, J., Liew, P.J. (2019). Material removal in ultrasonic abrasive polishing of additive manufactured components, *Applied Sciences,* Vol. 9, No. 24, Article No. 5359, doi: 10.3390/app9245359.
[26] Tan, K.L., Yeo, S.H. (2017). Surface modification of additive manufactured components by ultrasonic cavitation abrasive finishing, *Wear*, Vol. 378-379, 90-95, doi: 10.1016/j.wear.2017.02.030.
[27] Ichida, Y., Sato, R., Morimoto, Y., Kobayashi, K. (2005). Material removal mechanisms in non-contact ultrasonic abrasive machining, *Wear,* Vol. 258, No. 1-4, 107-114, doi: 10.1016/j.wear.2004.05.016.
[28] Whillock, G., Harvey, B.F. (1997). Ultrasonically enhanced corrosion of 304L stainless steel II: The effect of frequency, acoustic power and horn to specimen distance, *Ultrasonics Sonochemistry,* Vol. 4, No. 1, 33-38, doi: 10.1016/S1350-4177(96)00015-6.
[29] Virot, M., Chave, T., Nikitenko, S.I., Shchukin, D.G., Zemb, T., Möhwald, H. (2010). Acoustic cavitation at the water-glass interface, *Journal of Physical Chemistry C*, Vol. 114, No. 30, 13083-13091, doi: 10.1021/jp1046276.
[30] Couppis, E.C., Klinzing, G.E. (1974). Effect of cavitation on reacting systems, *AIChE Journal,* Vol. 20, No. 3, 485-491, doi: 10.1002/aic.690200308.
[31] Shchukin, D.G., Skorb, E., Belova, V., Möhwald, H. (2011). Ultrasonic cavitation at solid surfaces, *Advanced Materials,* Vol. 23, No. 17, 1922-1934, doi: 10.1002/adma.201004494.
[32] Bhosale, S.B., Pawade, R.S., Brahmankar, P.K. (2014). Effect of process parameters on MRR, TWR and surface topography in ultrasonic machining of alumina–zirconia ceramic composite, *Ceramics International,* Vol. 40, No. 8, Part B, 12831-12836, doi: 10.1016/j.ceramint.2014.04.137.
[33] Tzanakis, I., Eskin, D.G., Georgoulas, A., Fytanidis, D.K. (2014). Incubation pit analysis and calculation of the hydrodynamic impact pressure from the implosion of an acoustic cavitation bubble, *Ultrasonics Sonochemistry,* Vol. 21, No. 2, 866-878, doi: 10.1016/j.ultsonch.2013.10.003.